ISSN: 2755-0141

Japan Journal of Clinical & Medical Research

Review Article

Open Access

Near Infrared to Visible Upconversion Polarization Imaging Enabled by $Cs_2NaScCl_6$: Er^{3+} Composite Film

Henan Yang[1], Siyang Chen[2], Ye Wang[1], Cheng Ding[1], Kun Zheng[3], Jie Cao[1*], Bingkun Chen[1*] and Qun Hao[2]

[1]School of Optics and Photonics, Beijing Institute of Technology, Beijing 100081, China

[2]School of Electro - Optical Engineering, Changchun University of Science and Technology, Changchun 130022, China

[3]Yangtze Delta Region Academy of Beijing Institute of Technology, Jiaxing 314019, Zhejiang, China

***Corresponding author**
Jie Cao, Bingkun Chen, School of Optics and Photonics, Beijing Institute of Technology, Beijing 100081, China.

Received: May 25, 2026; **Accepted:** May 28, 2026; **Published:** June 09, 2026

Keywords: Lead-free Double Perovskite, $Cs_2NaScCl_6$: Er^{3+}, Upconversion Emission, Composite Film, Near Infrared Polarization Imaging

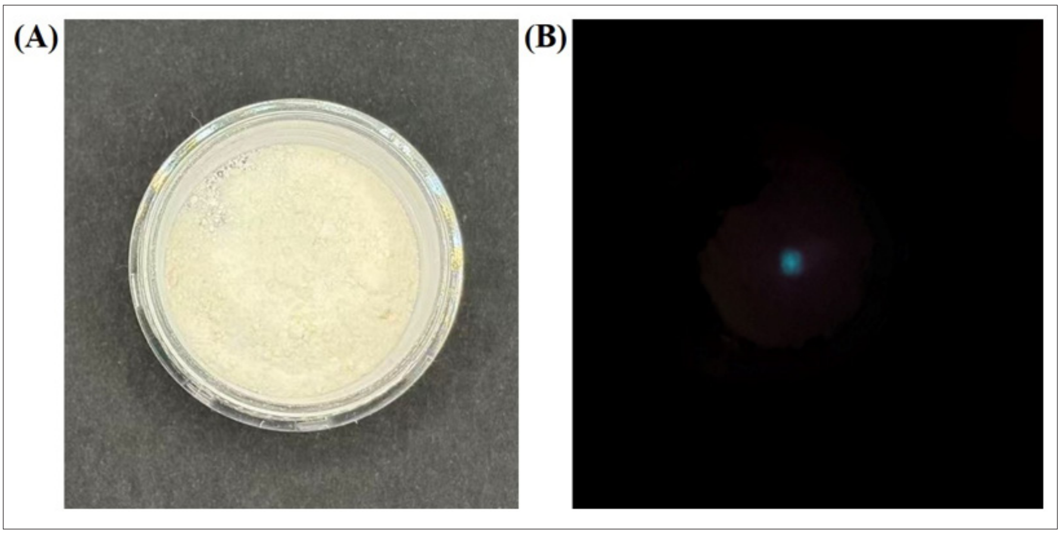

Figure 1: Photographs of the white powder obtained through the first step (just wet griding with deionized, not thermal treatment at 210 °C) under daylight (A) and 980 nm excitation (B)

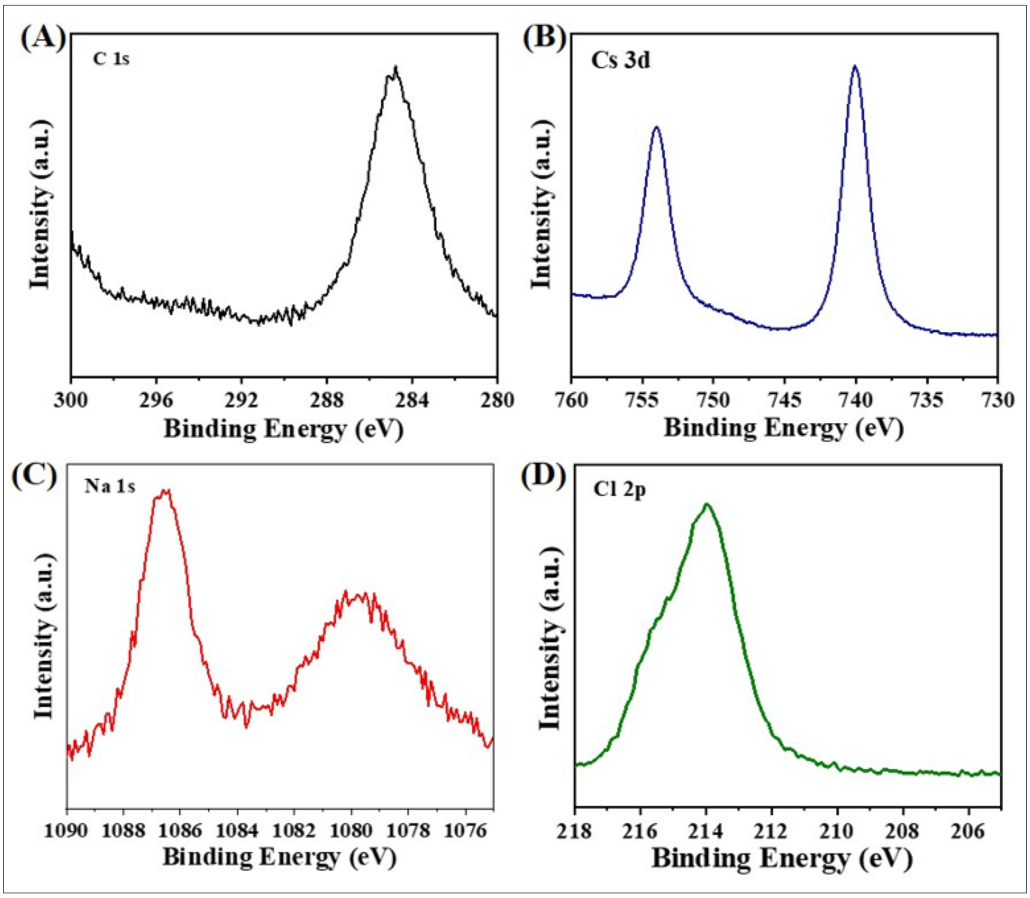

Figure 2: High-resolution XPS spectra of the $Cs_2NaScCl_6:Er^{3+}$ powder before mesh sieve process for elements C (A), Cs (B), Na (C), and Cl (D)

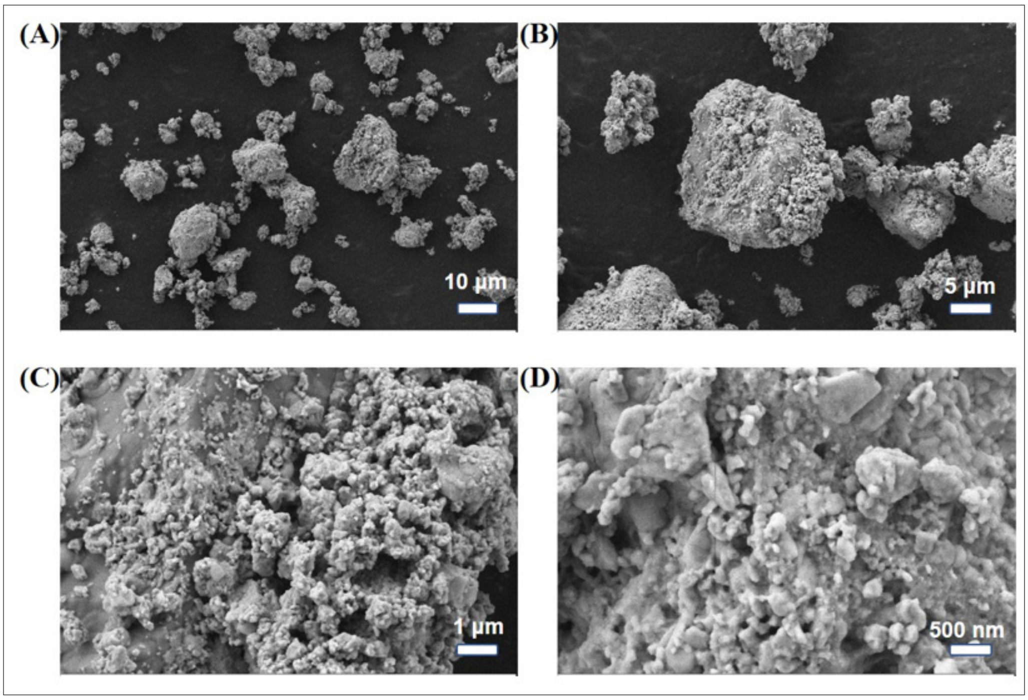

Figure 3: SEM images of the $Cs_2NaScCl_6:Er^{3+}$ powder before mesh sieve process with scale bars of 10 µm (A), 5 µm (B), 1 µm (C), and 500 nm (D)

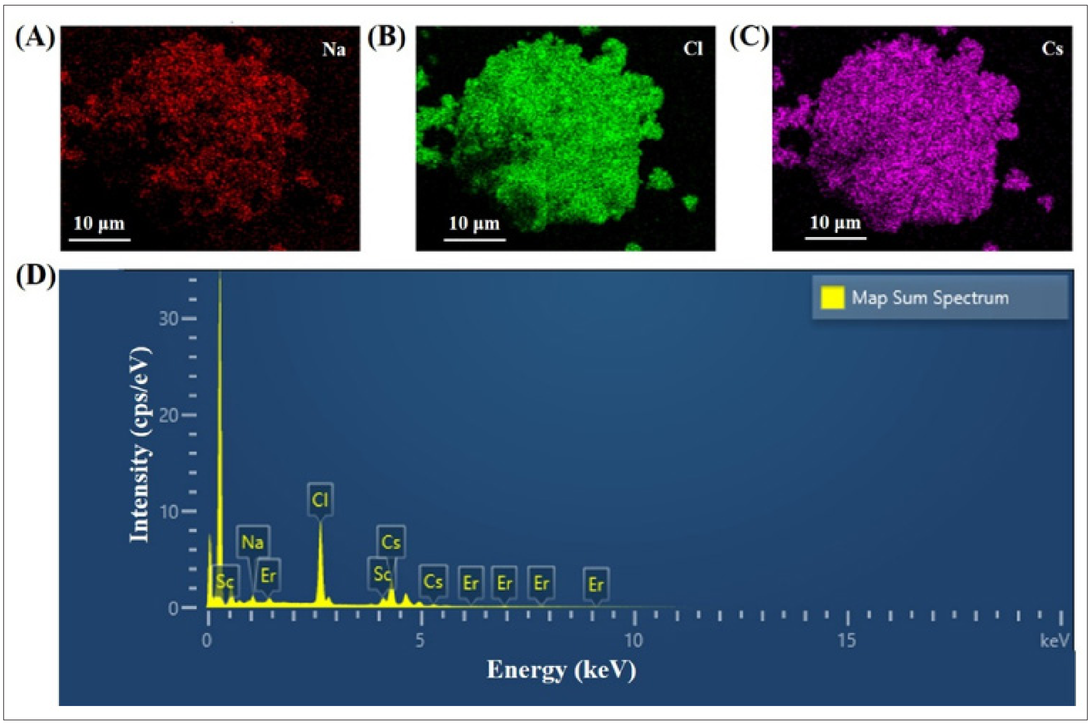

Figure 4: EDS mapping images of the $Cs_2NaScCl_6$:Er^{3+} powder before mesh sieve process for (A) Na, (B) Cl, (C) Cs and EDS spectrum shown in (D)

Table 1: Excitation Wavelengths, Emission Wavelengths, and PLQYs of Several Upconversion Emission Materials

Materials	Excitation Wavelength (nm)	Emission Wavelength (nm)	PLQY	Ref.
La_2O_2S: 9%Yb^{3+},1%Er^{3+}	977	820	5.83±0.87	[1]
BaY_2F_8: 20%Er^{3+}	1493	980	14.6 ± 1.5	[2]
$NaYF_4$: 20%Yb^{3+},2%Ho^{3+}, x%Ce^{3+}	970	641	-	[3]
$CaIn_2O_4$: Yb^{3+}/Ho^{3+}	980	545	5.5	[4]
Y2BaZnO_5: 7%Yb^{3+},0.5%Ho^{3+}	980	541	2.6	[5]
YF_3: Yb^{3+}, Tm^{3+}	970	312	5-	[6]
$NaErF_4$@$NaLuF_4$	1523	980	5.2	[7]
$NaYF_4$: Yb, Er@$NaGdF_4$: Nd@SiO_2-TiO_2	980	540	-	[8]
$NaYF_4$: Yb, Er, Tm	980	545	0.2	[9]
$LiY_{5/6}Yb_{1/6}F4$: 0.4 %Tm^{3+}	973	480	0.18±0.02	[10]
K_3YF_6: Yb^{3+}, Er^{3+}	980	546	0.3	[11]
$NaYF_4$@$NaYF_4$: Yb/Tm@$NaYF_4$ core-shell-shell NPs	980	450-500	13.0 ± 1.3	[12]
$Cs_2NaEr_xYb_{1-x}Cl_4$	980	665	12.9	[13]
$Cs_2NaScCl_6$:Er^{3+}	980	551	**5.98**	This work

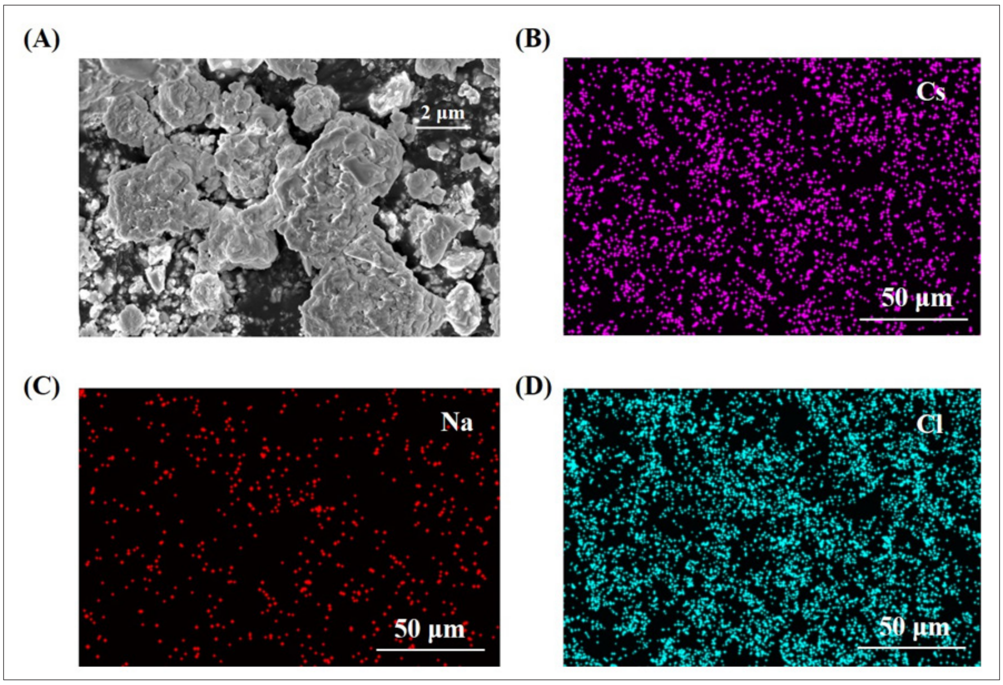

Figure 5: The magnified SEM image (A) and EDS mappings of Cs (B), Na (C), Cl (D) elements, for the 600-mesh sieved $Cs_2NaScCl_6$: Er^{3+} powder sample

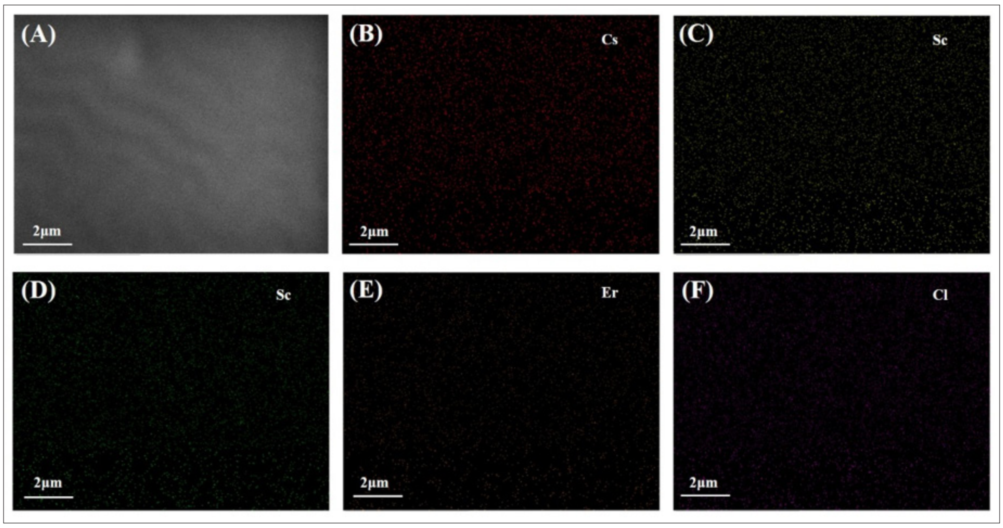

Figure 6: SEM image (A) and EDS mapping images of the $Cs_2NaScCl_6$: Er^{3+}/PDMS composite film, showing the elemental distributions of (B) Cs, (C) Na, (D) Sc, (E) Er, and (F) Cl, respectively

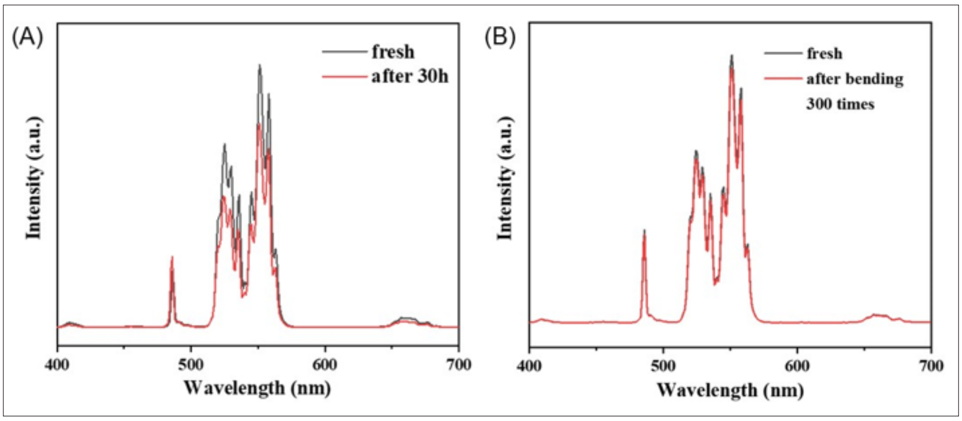

Figure 7: Upconversion photoluminescence spectrum of the $Cs_2NaScCl_6$:12% Er^{3+}/PDMS composite film (a) before and after continuous irradiation for 30 h; (b) before and after 300 bending cycles

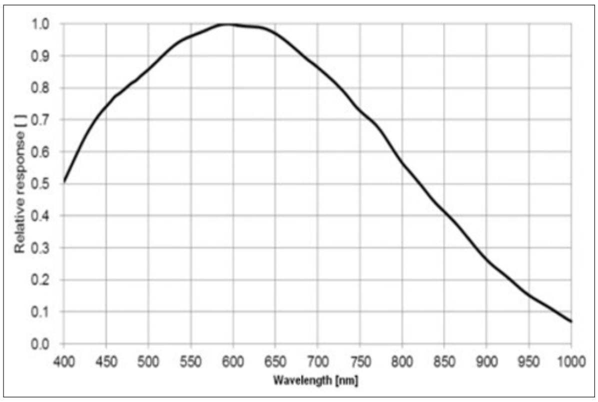

Figure 8: Detector's Response Curve Graph, cited from the operation manual of Hikvision polarization camera (Model: MV-CH050-10UP), which employs the Sony IMX250MZR polarization sensor chip

Table 2: Comparison of hardware parameters between the integrated detection system in this work and conventional near-infrared imaging systems (Under low-light and high-gain conditions)

Imaging system	SNR	DR	frame-rate range
This work	20.2 dB	71.0 dB	5-74 fps
Conventional near-infrared imaging system	18.6 dB	56.0 dB	30-60 fps

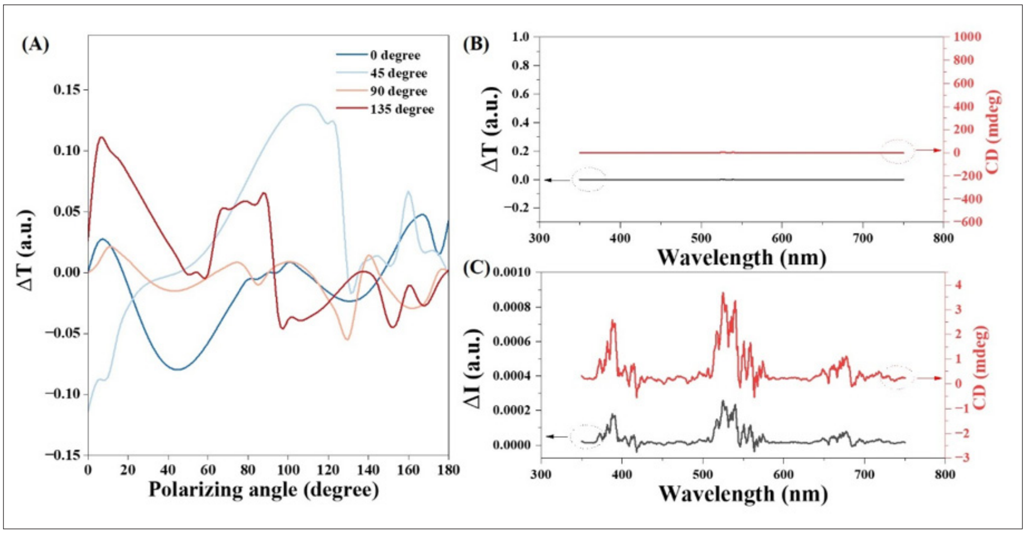

Figure 9: Polarization independent test of the as-fabricated $Cs_2NaScCl_6:Er^{3+}$ UCPL film. (A) The polarized transmitted intensity differences (ΔT) of the UCPL film and the ITO glass substrate under illumination with linearly polarized light at four incident angles (0°, 45°, 90°, and 135°). (B) ΔT and CD curves over wavelength. The black curve represents the ΔT of the UCPL film between LCP and RCP illumination over the wavelength range of 350-750 nm. The red curve denotes the CD of the UCPL film within the 350-750 nm wavelength range. (C) Enlarged curves corresponding to (B) for observing the subtle waveform

To investigate whether the $Cs_2NaScCl_6:Er^{3+}$ upconversion composite film used in this study exhibits polarization sensitivity and further eliminate the interference of the film on polarization imaging, we conducted a test to explore the effect of linear polarization angle on the light intensity of the UCPL composite film. The experimental setup is as follows: the experimental group adopted the $Cs_2NaScCl_6:Er^{3+}$-PDMS/ITO glass composite film, while the control group use pure ITO glass substrate. The test system is consisting of 980 nm laser, near-infrared polarizer, and polarization camera. The experimental procedure was set as follows: the polarizing polarizer was rotated from 0° to 180° with interval of 5°, and images of the experimental and control groups were taken at each step. The light intensity data were collected and the total light intensity was calculated. The linearly polarized light intensities in four directions detected under different polarization angles were analyzed, and the results are shown in Figure 5H and Figure S8. The polar coordinate system is shown in Figure 5H, illustrating that the upper and lower semicircle represent the results of the experimental group and the control group, respectively. Non-polarized property of the UCPL composite film was analyzed by observing the symmetry between the upper and lower semicircles. It can be seen that the light intensities shapes of the experimental group and the control group exhibit mirror symmetry at all polarization detection angles, which confirms that the UCPL composite film shows no polarization feature Figure S9(A) shows the difference in transmitted intensity between the upconversion film and the independent substrate under illumination with linearly polarized light at four polarization angles (0°, 45°, 90°, and 135°). The x-axis represents the different analyzer angles (from 0° to 180°). Figure S9(A) corresponds to the intensity difference between the curves of the same color in the upper semicircle and lower semicircle of Figure 5(H). Such discrepancies are identified as measurement errors with a random nature, and their magnitude indicates that the up-conversion film reported in this paper exhibits no polarization conversion or depolarization effect on linearly polarized light.

Although the content of circularly polarized light in nature is extremely low and negligible, this system does not collect circular polarization information, and circularly polarized light has no impact on the system. Nevertheless, as a precaution, we conducted a circular polarization detection on the film. In Figure S9(B-C), the black curve represents the transmitted light intensity difference ΔT over wavelength of the UCPL film upon illumination with left-handed circularly polarized light (LCP) and right-handed circularly polarized light (RCP). The red curve corresponds to the circular dichroism (CD) over wavelength of the UCPL film. The spectral range covers 350-750 nm. ΔI and CD formulas are given as follows:

$$\Delta T = T_{LCP} - T_{RCP} \qquad \text{(S1)}$$

$$CD = \frac{T_{LCP}^{1/2} - T_{RCP}^{1/2}}{T_{LCP}^{1/2} + T_{RCP}^{1/2}} \qquad \text{(S2)}$$

Herein, T_{LCP} and T_{RCP} denote the transmitted light intensities of the UCPL film under illumination with LCP and RCP, respectively. CD refers to the differential absorption between LCP and RCP. A positive value of ΔT indicates that the film induces a left-handed effect, whereas a negative value signifies a right-handed effect. The same principle applies to the CD value. Typically, the CD signal of strongly chiral materials reaches a magnitude of 1000 mdeg. As shown in Figure S9(B), the test results of the UCPL film in this study exhibit almost no spectral fluctuations at this scale. When the scale is magnified to that presented in Figure S9(C), as evidenced by the curves, a sharp increase in the left-handed effect emerges at approximately 390 nm and 540 nm; however, the magnitude of this effect is extremely small, remaining below 4 mdeg in all cases. This can be identified as baseline noise, confirming that the UCPL film exhibits no chiral characteristics.

References

1. Pokhrel M, Kumar GA, Sardar DK (2013) (Highly efficient NIR to NIR and VIS upconversion in Er3+ and Yb3+ doped in M2O2S (M = Gd, La, Y). Journal of Materials Chemistry A 1: 11595-11606.
2. Boccolini A, Favilla E, Tonelli M, Richards BS, Thomson RR (2015) Highly efficient upconversion in Er3+ doped BaY2F8 single crystals: dependence of quantum yield on excitation wavelength and thickness. Opt Express 23: A903- A915.
3. Gao W, Wang R, Han Q, Dong J, Yan L, et al. (2015) Tuning red upconversion emission in single LiYF4:Yb3+/Ho3+ microparticle. The Journal of Physical Chemistry C 119: 2349-2355.
4. Li T, Guo CF, Yang YM, Li L, Zhang N (2013) Efficient green up-conversion emission in Yb3+/Ho3+ co-doped CaIn2O4. Acta Materialia 61: 7481-7487.
5. Etchart I, Hernández I, Huignard A, Bérard M, Gillin WP, et al. (2011) Efficient oxide phosphors for light upconversion; green emission from Yb3+ and Ho3+ co-doped Ln2BaZnO5 (Ln = Y, Gd). Journal of Materials Chemistry 21: 1387-1394.
6. Chen D, Wang Y, Yu Y, Huang P (2007) Intense ultraviolet upconversion luminescence from Tm3+/Yb3+: β-YF3 nanocrystals embedded glass ceramic. Applied Physics Letters 91: 051920.
7. Wisser MD, Fischer S, Siefe C, Alivisatos AP, Salleo A, et al. (2018) improving quantum yield of upconverting nanoparticles in aqueous media via emission sensitization. Nano Letters 18: 2689-2695.
8. Zhang S, Dun S, Guo X, Zhang J (2022) A synergistic effect of NaYF4: Yb, Er@ NaGdF4: Nd@ SiO2 upconversion nanoparticles and TiO2 hollow spheres to enhance photovoltaic performance of dye-sensitized solar cells. Electrochimica Acta 421: 140435.
9. Jones CMS, Gakamsky A, Marques-Hueso J (2021) The upconversion quantum yield (UCQY): a review to standardize the measurement methodology, improve comparability, and define efficiency standards. Sci Technol Advanced Materials 22: 810-848.
10. Wen S, Zhou J, Zheng K, Bednarkiewicz A, Liu X, et al. (2018) Advances in highly doped upconversion nanoparticles. Nature Communications 9: 2415.
11. Shuai P, Yang D, Liao L, Guo Q, Mei L, et al. (2020) Preparation, structure and up-conversion luminescence properties of novel cryolite K3YF6:Er3+, Yb3+. RSC Advances 10: 1658-1665.
12. Li F, Tu L, Zhang Y, Huang D, Liu X, et al. (2024) Size-dependent lanthanide energy transfer amplifies upconversion luminescence quantum yields. Nature Photonics 18: 440-449.
13. Zhu Y, Pan G, Zhao J (2023) High-Efficiency Dual-Mode Polychromatic Emission of Rare-Earth-Based Double Perovskite with Low Phonon Energy toward High-Level Anti-Counterfeiting and Information Encryption. Advanced Optical Materials 11: 2202019.